Check for updates

Chemistry
A European
Journal

Chemistry Europe
European Chemical Societies Publishing

Accepted Article

Title: DNA Targeting Ru(II)-Polypyridyl Complex with Long-Lived 3IL Excited State as potential photodynamic therapy agent

Authors: Wuyang Hua, Gang Xu, Jian Zhao, Jiapeng Lu, Wenfang Sun, and Shaohua Gou

This manuscript has been accepted after peer review and appears as an Accepted Article online prior to editing, proofing, and formal publication of the final Version of Record (VoR). This work is currently citable by using the Digital Object Identifier (DOI) given below. The VoR will be published online in Early View as soon as possible and may be different to this Accepted Article as a result of editing. Readers should obtain the VoR from the journal website shown below when it is published to ensure accuracy of information. The authors are responsible for the content of this Accepted Article.

To be cited as: *Chem. Eur. J.* 10.1002/chem.202003031

Link to VoR: https://doi.org/10.1002/chem.202003031

WILEY-VCH

10.1002/chem.202003031

WILEY-VCH

DNA Targeting Ru(II)-Polypyridyl Complex with Long-Lived ^{3}IL Excited State as potential photodynamic therapy agent

Wuyang Hua‡,[a] Gang Xu‡,[a] Jian Zhao,*[a] Jiapeng Lu,[b] Wenfang Sun,*[b] and Shaohua Gou*[a]

Abstract: Subtle ligand modifications on Ru(II)-polypyridyl complexes may result in different excited-state characteristics, which provides the opportunity to tune their photo-physicochemical properties and subsequently change their biological functions. Here, a DNA targeting Ru(II)-polypyridyl complex (named **Ru1**) with highly photosensitizing ^{3}IL (intraligand) excited state was designed based on a classical DNA-intercalator $[Ru(bpy)_2(dppz)]\cdot 2PF_6$ by incorporation of dppz ligand tethered with pyrenyl group, which has 4 orders of magnitude higher potency than the model complex $[Ru(bpy)_2(dppz)]\cdot 2PF_6$ upon light irradiation. This study provides a facile strategy for the design of organelle-targeting Ru(II)-polypyridyl complex with dramatically improved photobiological activity.

Introduction

Photodynamic therapy (PDT) has been emerging as a promising cancer treatment modality, due to its excellent spatiotemporal selectivity, negligible side effects and noninvasiveness.[1] Upon light activation, photosensitizers (PSs) can exert anticancer effects by generating cytotoxic reactive oxygen species (ROS) via energy or electron transfer from the triplet excited state of the PSs to ground-state oxygen to kill cancer cells.[1c,1d,2] Therefore, PSs with long-lived triplet excited states are desired for PDT. Profiting from the rich photophysics and salient biological properties,[3] Ru(II)-polypyridyl complexes have been widely studied for their potential applications in organelle imaging, tumor diagnosis, chemotherapy and PDT.[4] The notable example is polypyridyl Ru(II)-dppz (dppz = dipyrido[3,2-a:2′,3′-c]phenazine) complexes, which have been widely known as DNA light switches and structure-specific DNA probes due to their two ^{3}MLCT (metal-to-ligand charge transfer) states (a luminescent ^{3}MLCT^{prox} state and a dark ^{3}MLCT^{dis} state) and strong DNA intercalation abilities.[5,6] Besides, a Ru(II)-polypyridyl complex, TLD1433, has successfully finished phase Ib clinical trial in 2018 and is currently in Phase 2 human clinical trial (ClinicalTrials.gov Identifier: NCT03945162) as a photosensitizer for bladder cancer PDT treatment, highlighting the great potential utility of Ru(II)-polypyridyl complexes in PDT.[6]

Cancer cells are more affected by DNA damage relative to normal cells due to their much faster division rates.[7] Therefore, DNA can serve as an effective target in PDT.[2a,8] Notably, it is generally accepted that binding of a PS to DNA is a vital step for efficient DNA photocleavage.[9] Consequently, Ru(II)-based PSs with DNA intercalation abilities could be favorable for PDT.[8,9] However, $[Ru(bpy)_2(dppz)]^{2+}$, a typical DNA light-switch complex, exhibited negligible photocytotoxicity due to its low singlet oxygen ($^1O_2$) generation efficiency.[10] To improve the photocytotoxicity of $[Ru(bpy)_2(dppz)]^{2+}$, Gasser and co-workers designed a number of $[Ru(bpy)_2(dppz)]^{2+}$ derivatives as PSs by incorporation of functional moieties on the dppz ligand.[11] This approach not only retained the DNA-binding affinity of the complexes, but also improved their photocytotoxicity and promoted the potential application of these complexes as PDT agents. However, the anticancer mechanism is still based on the similar ^{3}MLCT excited state as that in $[Ru(bpy)_2(dppz)]^{2+}$.

The lowest-energy triplet excited state (T_1) for $[Ru(bpy)_2(dppz)]^{2+}$ is ^{3}MLCT state,[6] which is less sensitive to O_2 due to its relatively short excited-state lifetime. One of the effective strategies to achieve the long-lived excited state of the Ru(II)-polypyridyl complex is to access the triplet intraligand (^{3}IL) state, which is extremely sensitive to O_2 or other excited-state quenchers.[3] Based on the reported work, we speculate that subtle modifications on the structures of Ru(II)-polypyridyl complexes may lead to different excited-state behaviors. This would provide an opportunity to tune the photo-physicochemical properties of the Ru(II)-polypyridyl complexes and improve their biological functions based on a rational design of the ligand. Furthermore, many Ru(II) complexes attached with pyrenyl groups were reported and showed greatly increased photocytotoxicity.[12] To examine that hypothesis, the pyrenyl group was selected as the functional moiety to lower the energy of the ^{3}IL state of $[Ru(bpy)_2(dppz)]^{2+}$ through substitution on the dppz ligand (Scheme 1). We hypothesize that introduction of the pyrenyl group would enable the access of the low-lying, long-lived pyrene-based ^{3}IL state of the resultant complex, and thus significantly improve the ROS production and photocytotoxicity of $[Ru(bpy)_2(dppz)]^{2+}$ without affecting its DNA-binding ability. Herein we report the synthesis, photophysics and photobiological activities of the new complex **Ru1** that has strong DNA intercalating ability and high photocytotoxicity. The possible mode of actions for this complex was also investigated. Besides the N^N Ru(II) complexes, plenty of cyclometalated Ru(II) complexes have been studied[13] and explored as photocytotoxic agents.[13a,b] For comparison with **Ru1**, complex **Ru2** (structure shown in Scheme 2) bearing the cyclometalating (C^N) analogue of dppz was synthesized and studied.

[a] W. Hua, Dr. G. Xu, Dr. J. Zhao, Dr. Z. Wang and Prof. S. Gou
Jiangsu Province Hi-Tech Key Laboratory for Biomedical Research and Pharmaceutical Research Center, School of Chemistry and Chemical Engineering
Southeast University, Nanjing 211189, China
E-mail: 101010898@seu.edu.cn (Prof. S. Gou) and zhaojianzhaokuan@163.com (Dr. J. Zhao)
[b] J. Lu and Prof. W. Sun
Department of Chemistry and Biochemistry
North Dakota State University, Fargo, North Dakota 58108-6050, USA
E-mail: wenfang.sun@ndsu.edu (Prof. W. Sun)
[‡] These authors contributed equally to this work.

Supporting information for this article is given via a link at the end of the document.

Accepted Manuscript

This article is protected by copyright. All rights reserved.

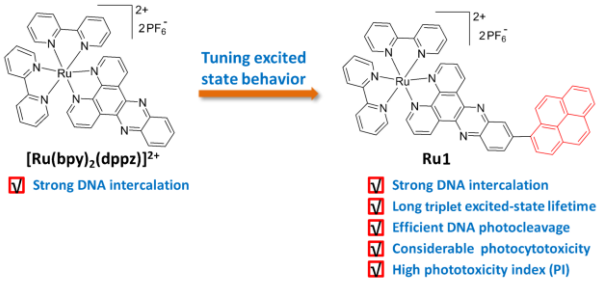

Scheme 1. Design Rationale for the DNA Targeting Ru(II)-polypyridyl PS (**Ru1**).

Results and Discussion

Synthesis and photophysical properties

Ru1 was synthesized by following the procedures shown in Schemes 2. The intermediate **1** was obtained by Suzuki coupling reaction. Then $[Ru(bpy)_2(1,10\text{-phenanthroline-5,6-dione})]\cdot 2PF_6$ was refluxed with intermediate **1** in methanol to afford **Ru1**. The cyclometalated organometallic Ru(II) analogue (**Ru2**) was prepared for comparison purpose, which existed as two stereoisomers (Scheme 2) and the mixture of isomers were used in this study. The synthesized complexes were characterized by ^1H and ^{13}C NMR spectroscopy along with elemental analysis and ESI-MS spectrometry.

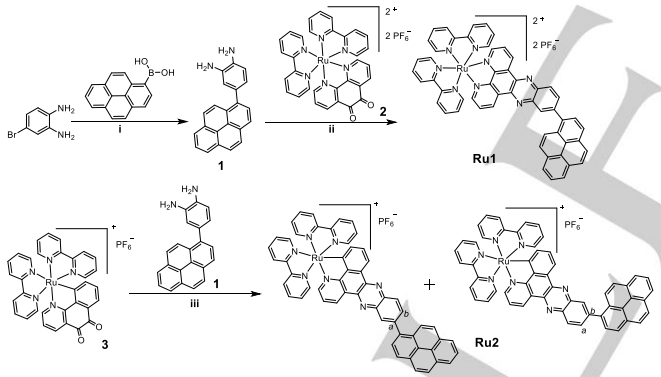

Scheme 2. Synthetic procedure of **Ru1** and **Ru2.** **i).** N_2, $Pd(PPh_3)_4$, K_2CO_3, toluene, ethanol, H_2O, reflux, yield 83 %; **ii).** N_2, methanol, reflux, yield 90 %; **iii.** N_2, methanol, reflux, yield 88 %.

The UV-Vis absorption and emission spectra of **Ru1** and **Ru2** were studied in CH_3CN and CH_2Cl_2, respectively. As shown in Figure 1a, **Ru1** exhibited a strong absorption in the region of 400 - 500 nm, with an absorption maximum at 450 nm (26900 M^{-1} cm^{-1}). The molar extinction coefficient of this band in **Ru1** is much stronger than those in $[Ru(bpy)_3]^{2+}$ (13000 M^{-1} cm^{-1})[10] and $[Ru(bpy)_2(dppz)]^{2+}$ (16300 M^{-1} cm^{-1})[10], indicating the enhanced light-harvesting ability of **Ru1** due to the extended π-conjugation via incorporation of pyrenyl group on dppz. Different from **Ru1**, two broad absorption bands were observed for **Ru2** at 370 - 450 nm and 450 - 600 nm, which can be assigned to the ^{1}MLCT/^{1}LLCT (ligand-to-ligand charge transfer) transitions involving the N^N and C^N ligands, respectively.[15,16]

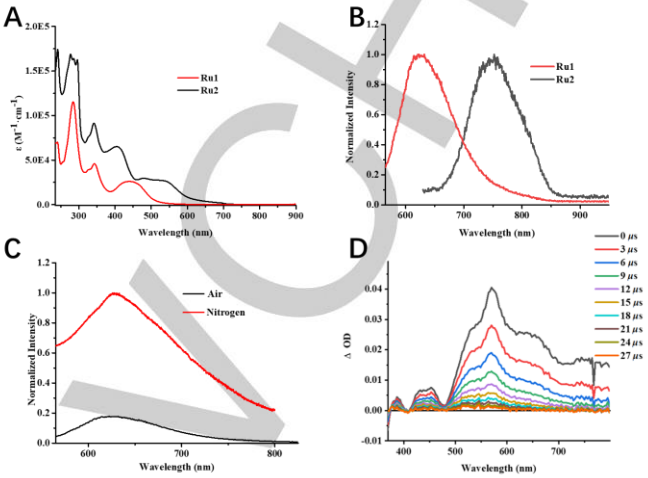

Figure 1. (A) UV-Vis absorption spectra of **Ru1** and **Ru2** in CH_3CN and CH_2Cl_2, respectively. (B) Emission spectra of **Ru1** (λ_{ex} = 534 nm) and **Ru2** (λ_{ex} = 590 nm) in CH_3CN and CH_2Cl_2, respectively. (C) Emission spectra of **Ru1** in aerated and deaerated acetonitrile. (D) Time-resolved triplet transient absorption spectra of **Ru1** in deaerated CH_3CN, λ_{ex} = 355 nm, A_{355} = 0.4 in a 1-cm cuvette.

The emission characteristics were investigated in acetonitrile for **Ru1** and in dichloromethane for **Ru2** due to its poor solubility in acetonitrile. As shown in Figure 1b, **Ru1** and **Ru2** emitted at 632 nm and 759 nm, respectively. Compared with $[Ru(bpy)_2(dppz)]\cdot 2PF_6$ and other pyrenyl-containing Ru(II) complexes,[12c,e] the maximum emission wavelength of **Ru1** showed a bathochromic shift, possibly attributing to the increased delocalization of the π-system of the ligand. However, **Ru2** exhibited a blue shift of the emission peak as compared with its analogue $[Ru(bpy)_2(ppy)]^+$ (825 nm in acetonitrile, ppy = 2-phenylpyridine).[13c] The emission of **Ru1** can be quenched by O_2 (Figrue 1c), indicating that the luminescence is phosphorescence. However, no obvious change in emission intensity of **Ru2** was observed between aerated and deaerated solutions (Figure S1a), probably owing to the short-lived emitting state. Based on the much red-shifted emission bands with respect to the corresponding excitation wavelengths, the sensitivity of the emission to air quenching, and referring to the similar Ru(II) complexes reported in the literature,[15] the observed emission should be phosphorescence from the triplet excited states for both **Ru1** and **Ru2**. However, the emission lifetimes of the two complexes were too short to be measured on our instrument. Considering the microsecond lifetime for the lowest triplet excited state (T_1) of **Ru1** discussed below, the emitting excited state in **Ru1** should not be its T_1 state. Ru(II) dyads tethered with π-expansive organic chromophores such as pyrene that possessed a long-lived nonemissive T_1 state and a high-lying emitting state have been reported previously.[10,16]

Accepted Manuscript

This article is protected by copyright. All rights reserved.

Table 1. Photophysical parameters of the related compounds.

Complexes	λ_{abs}/nm (ε/10^3 $M^{-1}cm^{-1}$)	λ_{em}/nm	Φ_{em} [a]	Φ_{Δ} [b]	τ_T/ μs [c]
$[Ru(bpy)_3]\cdot 2PF_6$	450(13.0), 423(9.8), 286(92.1)	621	0.10 [d]	0.81	0.2 [e]
$[Ru(bpy)_2(dppz)]\cdot 2PF_6$	445(16.3), 421(13.9), 366(17.9), 283(140.4)	622	0.08 [f]	0.16	0.8 [g]
Ru1	450(26.9), 343(4.6), 328(39.4), 284(115.3)	632	0.11	0.93	7.0 [h]
Ru2	533(27.0), 479(29.6), 404(65.1), 341(91.1), 297(160.3), 286(164.0)	759	-	-	-

[a] Luminescence quantum yield; [b] $^1O_2$ quantum yield in methanol; [c] Triplet excited-state lifetime; [d] Cited from Ref. 18; [e] Cited from Ref. 19; [f] Cited from Ref. 10; [g] Cited from Ref. 17; [h] In deaerated CH_3CN.

The triplet excited-state characteristics of **Ru1** and **Ru2** were further studied by the nanosecond transient absorption (TA) spectroscopy (Figure 1d). The triplet lifetime of **Ru1** deduced from the decay of TA signals was about 7 μs, almost 1 order of magnitude longer than that of $[Ru(bpy)_2(dppz)]^{2+}$ (0.8 μs).[17] This manifests that introduction of the pyrenyl group to $[Ru(bpy)_2(dppz)]^{2+}$ greatly prolongs its triplet excited-state lifetime. However, the triplet excited-state lifetime of **Ru2** was unable to be reliably detected due to its instability upon 355-nm laser excitation (Figure S1b).

Density functional theory calculation (DFT)

DFT calculations were performed to understand the parentage of the T_1 state[15] of **Ru1** by calculating the spin density surface. As shown in Figure 2, the triplet spin density of T_1 is exclusively distributed on the pyrene and dppz motifs, which makes the T_1 state $^3\pi,\pi^*$ in nature and thus longer lived. In contrast, the spin density surface of $[Ru(bpy)_2(dppz)]^{2+}$ is delocated on the Ru metal center and the dppz and bipyridine ligands, indicating a ^{3}MLCT/^{3}LLCT configuration in its T_1 state.

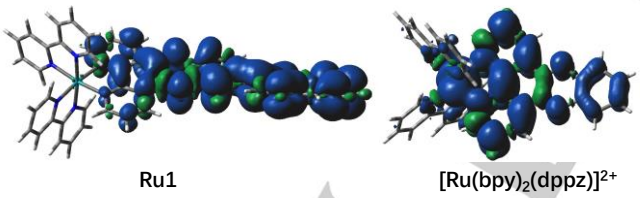

Figure 2. Isosurfaces for the spin density of **Ru1** and $[Ru(bpy)_2(dppz)]^{2+}$ at their optimized triplet-state geometries.

Reactive oxygen species (ROS) generation

The ROS generation abilities of the Ru(II) complexes were determined using a chemical trapping method by monitoring the decrease of absorption of 1,3-diphenylisobenzofuran (DPBF) at 410 nm in methanol.[10] As we expected, **Ru1** greatly reduced the absorption of DPBF at 410 nm upon 460-nm light irradiation (Figure S2d), whereas a faint decrease of DPBF absorbance was observed for $[Ru(bpy)_2(dppz)]\cdot 2PF_6$, suggesting that **Ru1** is

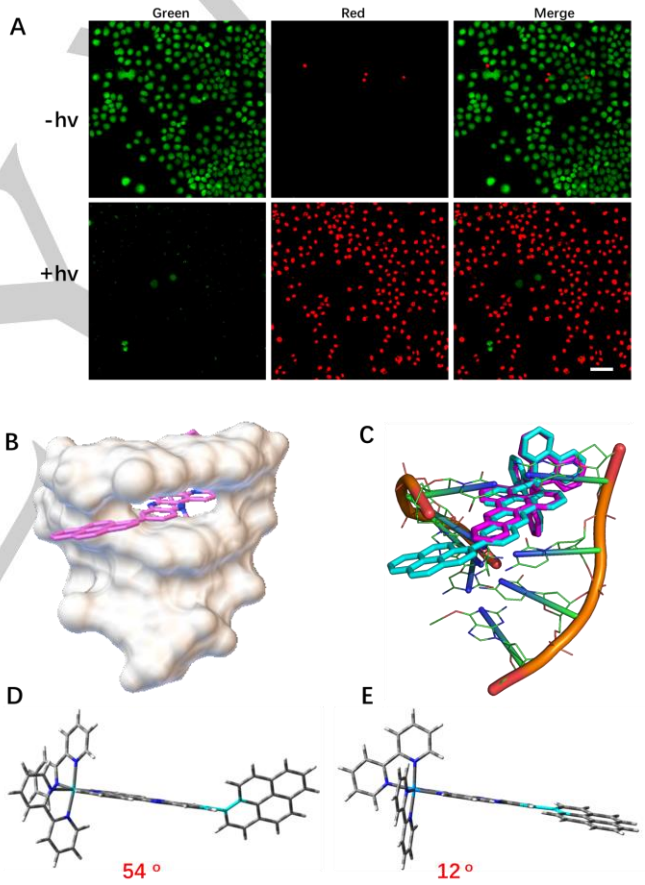

Figure 3. (A) Live/dead cell co-staining assays using calcein AM and propidium iodide as fluorescence probes. Cells were incubated with 0.05 μM of **Ru1** for 4 h and then with the fluorescence probes for 30 min without light irradiation (-hv). The cells were incubated with 0.05 μM of **Ru1** for 4 h followed by 460-nm light (6.0 mW/cm^2) irradiation for 2 min and then incubated with fluorescence probes for 30 min (+hv). Calcein AM and propidium iodide (5 μM, respectively) were used as fluorescence probes. Green channel: λ_{ex} = 488 nm, λ_{em} = 500-540 nm. Red channel: λ_{ex} = 561 nm, λ_{em} = 600-640 nm. Scale bar = 80 μm. (B, C) Molecular docking study of (B) **Ru1** and (C) Overlapped **Ru1** and $[Ru(bpy)_2dppz]^{2+}$ with DNA. (D, E) Dihedral angles between the pyrenyl substituent and the phen motif of **Ru1** (D) before and (E) after docking with DNA.

Accepted Manuscript

This article is protected by copyright. All rights reserved.

Table 2. IC_{50} values of the Ru(II) complexes against A549 and MCF-7 cancer cell lines.

Complex	A549			MCF-7		
	Dark (μM)	Light (μM)	PI[a]	Dark (μM)	Light (μM)	PI
Ru1	10.3 ± 1.2	0.010 ± 0.001	1030	13.4 ± 1.5	0.004 ± 0.001	3350
Ru2	10.9 ± 0.2	8.30 ± 0.71	1.3	15.2 ± 1.7	12.2 ± 1.3	1.2
$[Ru(bpy)_3]\cdot 2PF_6$	57.6 ± 3.5	8.30 ± 0.4	6.9	53.9 ± 4.3	7.20 ± 0.5	7.5
$[Ru(bpy)_2(dppz)]\cdot 2PF_6$	168 ± 9.8	147 ± 2.3	1.1	200 ± 4.5	152 ± 3.0	1.3
Cisplatin	5.40 ± 0.3	4.92 ± 0.2	1.1	6.20 ± 0.4	6.60 ± 0.6	0.9

[a] PI = dark IC_{50} value/Light IC_{50} value.

capable of producing ROS more efficiently than $[Ru(bpy)_2(dppz)]\cdot 2PF_6$. The ROS quantum yields of **Ru1** and $[Ru(bpy)_2(dppz)]\cdot 2PF_6$ were measured to be 0.93 and 0.16 (Table 1), respectively, using $[Ru(bpy)_3]\cdot 2PF_6$ (Φ_s=0.81)[20] as the standard. The ROS quantum yields of $[Ru(bpy)_2(dppz)]\cdot 2PF_6$ was in good agreement with those reported in the literature.[10] In contrast, no obvious changes of DPBF absorbance were observed for **Ru2**, implying the negligible ROS generation under the test condition. The drastic difference in ROS generation efficiency of **Ru1** and **Ru2** likely reflects the difference in the T_1 lifetimes of these two complexes. The longer the T_1 lifetime, the higher the ROS generation efficiency.

In vitro photocytotoxicity

The cytotoxicity and photocytotoxicity of **Ru1** and **Ru2** were evaluated against A549 (human pulmonary adenocarcinoma cell) and MCF-7 (human breast cancer cell) cancer cell lines by MTT assay,[2b] together with $[Ru(bpy)_3]\cdot 2PF_6$, $[Ru(bpy)_2(dppz)]\cdot 2PF_6$ and cisplatin as controls. Initially, the concentrations ranging from 0.25 to 200 μM were chosen for the study. Unexpectedly, all the cancer cells were killed by **Ru1** even at the lowest concentration (0.25 μM) upon 460-nm irradiation (6.0 mW/cm^2, 3.6 J/ cm^2), demonstrating the dramatic photocytotoxicity of **Ru1**. Therefore, **Ru1** was further tested with concentrations in the range of 0.001 - 0.125 μM.

According to the IC_{50} values (Table 2), **Ru1** exhibited markedly high phototoxic activities against A549 and MCF-7 cancer cells with exceptionally large phototherapeutic indices (PIs) of 1030 and 3004, respectively. Notably, **Ru1** possesses the same core structure as that of $[Ru(bpy)_2(dppz)]\cdot 2PF_6$, except for a pyrenyl group pendant on the skeleton of dppz. This structural modification enables **Ru1** to be 4 orders of magnitude more potent than $[Ru(bpy)_2(dppz)]\cdot 2PF_6$ under 460-nm light irradiation. In contrast, **Ru2** produced no discernible phototoxic activity due to its negligible ROS generation efficiency. Collectively, incorporation of a pyrene moiety on the dppz ligand of $[Ru(bpy)_2(dppz)]\cdot 2PF_6$ allows for the access of the long-lived ^{3}IL state of the resultant complex and greatly increases its triplet excited-state lifetime, which in turn significantly improved the phototoxicity of the new complex.

Live/dead cell co-staining assay

Photocytotoxicity of **Ru1** was further studied by live/dead cell co-staining assay.[21] Calcein AM and propidium iodide (PI) were used to label the living and dead cells, respectively. Because of the stronger photocytotoxicity of **Ru1** toward the MCF-7 cell line, this assay and the following photobiological studies were carried out only on the MCF-7 cell line. As shown in Figure 3a, very few cell death was observed for MCF-7 cells without light irradiation, whereas cells were almost killed upon light irradiation as revealed by the intense red fluorescence. This experiment further demonstrates the potent PDT capability of **Ru1**.

DNA interactions

DNA is an effective cancer therapeutic target for metal-based complexes. In many cases photoinduced DNA damage is responsible for the photobiological activity of Ru(II)-polypyridyl PSs.[8] Since $[Ru(bpy)_2dppz]\cdot 2PF_6$ was reported to be able to interact with DNA,[10,11] the DNA binding and photodamaging properties of the new complexes **Ru1** and **Ru2** were explored. DNA binding abilities of the complexes were studied by the fluorescence competitive binding experiments.[22,23] As shown in Figure S3, the emission intensities of DNA-bound ethidium bromide (EtBr) were greatly decreased upon addition of **Ru1**, **Ru2** and $[Ru(bpy)_2(dppz)]\cdot 2PF_6$, possibly attributing to the replacement of EtBr by these Ru(II) complexes. However, It is worth noting that the Ru(II) complexes can absorb the excitation light in this assay. With the increased amount of the Ru(II) complexes, the excitation light could be absorbed, resulting in fluorescence quenching.

To further confirm the interactions of the Ru(II) complexes with DNA, electronic absorption titration was conducted with results shown in Figure S4. Addition of ctDNA caused hypochromicity in the absorption spectra of all Ru(II) complexes, probably due to the intercalations of the Ru(II) complexes with ctDNA.[4l] Red shifts were also observed in the spectra of $[Ru(bpy)_2(dppz)]\cdot 2PF_6$ and **Ru1** treated group. The DNA interaction was further confirmed by circular dichroism (CD) spectrum. As prescented in Figure S5A, addition of **Ru1** and **Ru2** dramatically changed the CD spectrum of ctDNA, demonstrating that these two complexes effectively binded with DNA.

Accepted Manuscript

This article is protected by copyright. All rights reserved.

DNA intercalation was proven by the DNA melting temperature assay.[12c] As shown in Figure S5B, the DNA melting temperatures of $[Ru(bpy)_2(dppz)]\cdot 2PF_6$, **Ru1,** and **Ru2** treated groups were 69 ℃, 66 ℃, and 65 ℃, respectively, which were higher than that of free ctDNA (T_m = 61 ℃), demonstrating the intercalation effect of **Ru1,** and **Ru2.** It was reported that intercalation of the ligand into DNA could cause significant viscosity increase of the DNA solution.[12c] Therefore, viscosity of the DNA solutions treated with the Ru(II) complexes was carried out. As shown in Figure S5C, with the addition of Ru(II) complexes, the viscosity of ctDNA increased apparently, further confirming that **Ru1** and **Ru2** binded to DNA via intercalation.

The DNA binding mode of **Ru1** was further studied by molecular docking using AutoDock 4.2.[24] As shown in Figures 3b and 3c, the most stable binding conformation of **Ru1** and DNA manifested that **Ru1** can intercalate with DNA base pairs. Moreover, **Ru1** overlapped well with the co-crystallized $[Ru(bpy)_2(dppz)]^{2+}$ in the DNA crystal structure, indicating the similar binding mode of **Ru1** to that of $[Ru(bpy)_2(dppz)]^{2+}$ (Figure 3c).[24b] Importantly, the intercalation induced conformational constrain of **Ru1**, which reduced the dihedral angle between the pyrenyl substituent and the dppz ligand from 54° in the optimized ground-state geometry for the unbound **Ru1** to 12° upon binding with DNA. This result indicates that intercalation increased the coplanarity of the pyrenyl-substituted dppz ligand in **Ru1** (Figure 3d and 3e), which would increase the $^3\pi,\pi^*$ configuration in the T_1 state and prolong the excited-state lifetime of **Ru1**. This change would facilitate its application for PDT.

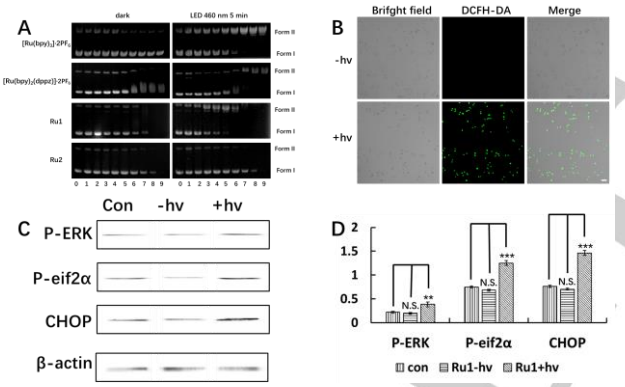

Figure 4. (A) Agarose gel mobility pattern of pBR322 plasmid DNA incubated with the Ru(II) complexes at the concentrations of 0 (0 μM), 1 (0.39 μM), 2 (0.78 μM), 3 (1.56 μM), 4 (3.12 μM), 5 (6.25 μM), 6 (12.5 μM), 7 (25.0 μM), 8 (50.0 μM), 9 (100 μM), respectively. The pBR322 DNA incubated with the complexes was then irradiated with a 460-nm LED light (6.0 mW/cm^2) for 5 min and incubated overnight. (B) Cell images of MCF-7 cells treated with **Ru1** and DCFH-DA. (-hv) The cells were loaded with **Ru1** (0.05 μM) and DCFH-DA (5 μM) successively without light irradiation. (+hv) The cells were incubated with **Ru1** (0.05 μM) for 4 h, loaded with DCFH-DA (5 μM) and irradiated with 460-nm light for 2 min. λ_{ex} = 488 nm. λ_{em}=520-550 nm. Scale bar: 80 μm. (C, D) Results of ER stress evaluation of MCF-7 cells after treatment with **Ru1**. (C) Blots; (D) Relative gray intensity analysis. MCF-7 cells were incubated with 0.05 μM of **Ru1** for 4 h and irradiated by 460-nm light (6.0 mW/cm^2) for 2 min. The cells were further incubated for 4 h before evaluation. Relative gray intensity = (gray intensity of indicated protein)/(gray intensity of β-actin). The data are representative of three independent experiments and the mean ± S.D. is shown. ***p < 0.001, **p < 0.01. Two-sided Student's t-test.

The DNA photocleavage abilities of **Ru1** and **Ru2** were investigated by agarose gel electrophoresis, with pBR322 plasmid DNA as the target and $[Ru(bpy)_3]\cdot 2PF_6$ and $[Ru(bpy)_2(dppz)]\cdot 2PF_6$ as the controls. As revealed in Figure 4a, without light irradiation, no changes were observed for the $[Ru(bpy)_3]\cdot 2PF_6$ group. However, the intensity of plasmid DNA bands gradually disappeared with the increased concentrations of **Ru1** and **Ru2**, indicating that these complexes effectively inhibited the intercalation of EtBr into plasmid DNA. This result is in accordance with the result from the EtBr competitive binding experiment. It should be noted that although $[Ru(bpy)_3]\cdot 2PF_6$ possesses weak DNA binding ability and $[Ru(bpy)_2(dppz)]\cdot 2PF_6$ has low ROS generation efficiency (as discussed in previous sections), they are still able to induce DNA damage at high concentrations upon 460-nm irradiation. **Ru1** showed efficient DNA photocleavage upon irradiation, which induced a complete single-strand break in pBR322 DNA at the concentration of 6.25 μM (drug-to-nucleotide ratio: 0.041) and thus led to the formation of nicked circular form (Form II) of the DNA. In contrast, **Ru2** did not show any observable DNA cleavage under 460-nm light irradiation because of its inability to form ROS. These results demonstrate that a strong DNA binding ability and a high $^1O_2$ generation efficiency are the two essential factors for efficient DNA photocleavage.

Cellular ROS production

The *in vitro* ROS generation of **Ru1** was evaluated in MCF-7 cells with DCFH-DA (2,7-dichlorodihydrofluorescein diacetate) as the ROS probe. As shown in Figure 4b, no ROS signal was observed for **Ru1** treated MCF-7 cells without irradiation. On the contrary, an obvious green fluorescence was observed upon 460-nm irradiation, demonstrating the effective ROS generation ability of **Ru1** in MCF-7 cells.

Endoplasmic reticulum stress activation

Endoplasmic reticulum (ER) is vulnerable to ROS damage.[25] To evaluate whether **Ru1** induced the ER stress upon light activation, expression levels of the phosphorylated RNA-dependent protein kinase-like endoplasmic reticulum kinase (P-ERK), phosphorylated eukaryotic initiation factor 2α (P-eif2α)[25c] and C/EBP homologous protein (CHOP) in MCF-7 cells were measured by western blot assay. As shown in Figures 4c and 4d, **Ru1** up-regulated the expression of all the tested proteins upon light irradiation, indicating that **Ru1** can induce ER stress via P-ERK/eif2α pathway in cancer cells.

Accepted Manuscript

This article is protected by copyright. All rights reserved.

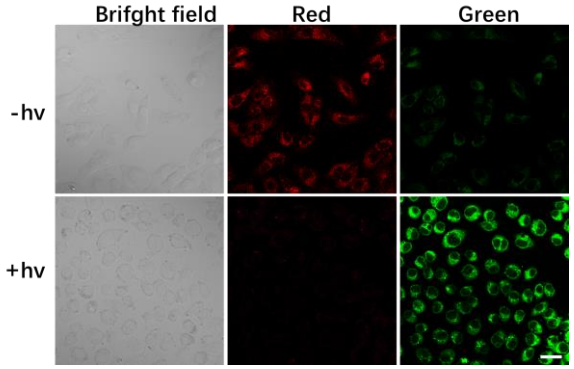

Figure 5. Cell images of MCF-7 cells treated with 0.05 μM of **Ru1** for 4 h in dark (-hv) or irradiated with 460-nm light (6.0 mW/cm^2) for 2 min (+hv) and loaded with JC-10. Red channel: λ_{ex} = 561 nm, λ_{em} = 580-680 nm. Green channel: λ_{ex} = 488 nm, λ_{em} = 500-540 nm. Scale bar: 20 μm.

Mitochondrial membrane potential change

Mitochondria is another common target for PDT. To assess whether PDT using **Ru1** caused mitochondrial damage, the mitochondrial membrane potential (MMP) change of MCF-7 cells was evaluated with or without light irradiation.[26] When the MMP is at a high level, JC-10 aggregates in the matrix of mitochondria, resulting in a red fluorescence. Once the MMP decreases, JC-10 exists as the monomer and emits green fluorescence. As shown in Figure 5, the **Ru1** group showed red emission without light irradiation. However, an intense green fluorescence from the MCF-7 cells was observed after light irradiation, indicating the decrease of MMP in MCF-7 cells. The loss of MMP should be attributed to the significant photocytotoxicity of **Ru1**.

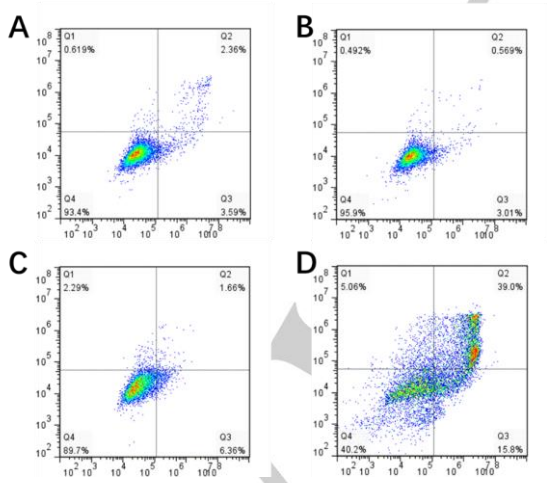

Figure 6. Apoptosis inducing property of (A) Control in dark. (B) Control with irradiation. (C) **Ru1** in dark. (D) **Ru1** with irradiation. The cells were incubated with 0.05 μM of **Ru1** for 4 h and irradiated by 460-nm (6.0 mW/cm^2) light for 2 min. MCF-7 cells were stained by Annexin V-FITC/PI. The Y-axis shows the PI-labeled population and the X-axis shows FITC-labeled Annexin V-positive cells.

Cell death pathways

To evaluate the cell death pathways induced by **Ru1** PDT on MCF-7 cells, flow cytometry assay was conducted with or without light irradiation. As revealed in Figure 6, 460-nm light irradiation alone had no effect on the cell death rates (apoptosis and necrosis). Negligible cell death rates were observed for **Ru1**-treated MCF-7 cells without light irradiation. Once light irradiation was conducted, the cell death rates induced by **Ru1** were greatly increased to 59.9%, further confirming the dramatic photocytotoxicity of **Ru1**. This result also indicates that apoptosis, especially late apoptosis is the dominant cell death pathway.

Conclusions

A Ru(II)-polypyridyl complex **Ru1** was designed by tethering the pyrenyl substituent to the dppz ligand on [Ru(bpy)$_2$(dppz)]·2PF$_6$. Both spectroscopic study and DFT calculation revealed that **Ru1** possessed a long-lived ^{3}IL T_1 state. In vitro PDT studies indicated that **Ru1** displayed a remarkable photocytotoxicity against A549 and MCF-7 cells, with IC_{50} values of 10 and 4 nM, respectively, which led to exceptionally large phototherapeutic indices (PIs) of 1030 and 3004, respectively. Notably, **Ru1** was 4 orders of magnitude more potent than [Ru(bpy)$_2$(dppz)]·2PF$_6$ upon light irradiation, demonstrating the dramatic improvement of the photobiological activity via incorporation of the pyrenyl substituent to [Ru(bpy)$_2$(dppz)]·2PF$_6$. Biological studies indicated that **Ru1** induced cell death through photoinduced DNA damage, ER stress and MMP change. This study manifests that the photophysical and biological activities of the organelle-targeting Ru(II)-polypyridyl complexes can be significantly altered via subtle ligand structural modifications. This design strategy could stimulate the development of more efficient organelle-targeting Ru(II)-polypyridyl complexes with improved excited-state properties for potential clinical PDT applications.

Experimental Section

The details for complex synthesis, photophysical studies are provided in the Supporting Information.

Photophysical measurements

Ru1 and **Ru2** were dissolved in CH_3CN and CH_2Cl_2, respectively. The UV-Vis absorption measurements were conducted on a Varian Cary 50 spectrophotometer. The emission spectra of **Ru1** and **Ru2** were recorded on a Horiba Jobin-Yvon FluoroMax-4 fluorometer/phosphorometer. The solutions were degassed with N_2 for 30 min prior to measurement. The excitation wavelength was 534 nm for **Ru1** and 590 nm for **Ru2**. The time-resolved triplet transient absorption spectra and triplet lifetimes were measured on an Edinburgh LP920 laser flash photolysis spectrometer. The excitation light was the third harmonic output (355 nm) of a Brilliant Nd:YAG laser with the repetition being set up to 1 Hz. The solutions were degassed with N_2 for 30 min. The concentrations of sample solutions were adjusted to reach an absorbance of 0.4 in a 1-cm cuvette at 355 nm.

DPBF assay to evaluate $^1O_2$ production of Ru1 in solution

Accepted Manuscript

This article is protected by copyright. All rights reserved.

60 μM DPBF in methanol and 10 μM **Ru1** in methanol were mixed in an equal volume. Then the solution was taken to record the UV-Vis absorption spectrum after irradiated by 460-nm LED light (2.6 mW/cm^2) for every 15 s. The $^1O_2$ quantum yield was calculated by using $[Ru(bpy)_3]^{2+}$ (Φ_s=0.81) as the standard following the equation:

$$\Phi_x=\Phi_s\cdot S_x\cdot F_s/(S_s\cdot F_x)$$

The subscripts x and s refer to the sample and $[Ru(bpy)_3]^{2+}$, respectively. S stands for the slope of plot of the -ln(Abs 410 nm) *vs* irradiation time (in this study, we chose the initial 5 points). F stands for the absorption correction factor, $F=1-10^{-OD}$. OD represents the optical density at 460 nm.

MTT assay

In vitro anticancer activity of **Ru1** and **Ru2** against A549 and MCF-7 cancer cells were carried out by the MTT assay. Cancer cells were plated in 96-well plates at density of 10^5/mL per well. After an overnight culturing, cells were exposed to culture medium containing **Ru1**, **Ru2**, $[Ru(bpy)_3]\cdot 2PF_6$, $[Ru(bpy)_2dppz]\cdot 2PF_6$ and Cisplatin separately at a series of concentrations and incubated overnight. Then the cells were exposed to 460-nm light (6.0 mW/cm^2) for 10 min or not. Then the cells were incubated for further 24 h. After that, 10 μL of MTT solution was added and the medium was removed. After a 4 h incubation, 130 μL of DMSO was added then the cells was taken to microplate reader to record the absorption at 490 nm.

Cellular ROS produce ability of Ru1

To a glass bottom cell culture dish containing MCF-7 cells, 1 μL of **Ru1** (50 μM) in PBS (10 mM, pH=7.4, containing 10% DMSO) was added into 999 μL of culture medium to make the final concentration of **Ru1** as 0.05 μM and the cells was cultured for 4 h. Then the medium was removed, and the cells was washed by 1 mL PBS (10 mM, pH=7.4). After that, 1 mL of DCFH-DA solution (5 μM) was added and the cells were incubated for 10 min. Then the cells were irradiated by 460-nm light (6.0 mW/cm^2) for 2 min and washed by PBS (10 mM, pH=7.4), followed by detection with LSCM. The excitation wavelength was 488 nm. The emission fluorescence was collected at 500-600 nm.

Mitochondrial membrane potential decrease

MCF-7 cells in a glass bottom cell culture dish were treated with 0.05 μM of **Ru1** for 4 h. For irradiation experiment, the cells were triggered by 460-nm LED light (6.0 mW/cm^2) for 2 min. The medium was removed, and the cells were washed with 1 mL of PBS (10 mM, pH=7.4). Then 500 μL of JC-10 working solution was added to each dish. After a 15-min incubation, the cells were washed by PBS (10 mM, pH=7.4) and moistened with 300 μL deionized water. The cells were detected by LSCM. The excitation and emission wavelength for monomer was 488 nm and 500-540 nm. For aggregation, the excitation and emission wavelength were 561 nm and 580-640 nm.

Cell apoptosis analysis

MCF-7 cells were treated with 0.05 μM of **Ru1** 4 h. For irradiated group, the cells were triggered by 460-nm LED light (6.0 mW/cm^2) for 2 min. After further incubated for 1 h, cells were collected by trypsinization and washed with PBS (10 mM, pH=7.4) twice, and then suspend cells in 1× Binding Buffer (0.1 M Hepes/NaOH (pH=7.4), 1.4 M NaCl, 25 mM $CaCl_2$). Then the cells were stained with FITC Annexin V (100 ng/mL) and propidium iodide (PI, 2 μg/mL) using annexin-V FITC apoptosis kit for 30 min at room temperature (25 ℃) in dark. The apoptosis ratio was quantified by system software (Cell Quest; BD Biosciences).

Live/dead cell co-staining assay

MCF-7 cells were treated with 0.05 μM of **Ru1** and incubated in a glass bottom dish for 4 h. For irradiated group, the cells were triggered by 460-nm LED light (6.0 mW/cm2) for 2 min. The cells were further incubated for 1 h. Then the culture medium was removed, and the cells were washed with PBS (10 mM, pH=7.4). Next, the cells were incubated with live/dead cell fluorescence probes calcein AM and propidium iodide (5 μM respectively) for 30 min, followed by washing with PBS (10 mM, pH = 7.4). Finally, the cells were detected by LSCM. For the red channel, the sample was excited with a 561 nm laser and the emission was collected at 600-640 nm. For the green channel, the excitation wavelength was 488 nm and the emission was detected at 500-540 nm.

Agarose gel electrophoresis study

pBR322 plasmid DNA (0.1 μg/μL) was incubated with complexes at a concentration of 0, 0.39, 0.78, 1.56, 3.12, 6.25, 12.50 and 25.00, 50.00 and 100.00 μM, separately. For irradiated group, the samples were triggered by 460-nm LED light (6.0 mW/cm^2) for 5 min. Then the samples were incubated at 37 ℃ in dark overnight. After that, the samples were loaded with loading buffer (10 %, v/v) and separated by agarose gel (100 V, 1h). Next, the gel was incubated by ethidium bromide (0.75 μg/mL) aqueous solution for 30 min. Finally, the gel was washed by water and taken to gel imaging system.

DNA-EB fluorescence competing experiments

1.5 mL of ctDNA (50 μM) and 1.5mL of EB (50 μM) were mixed. After every 2 μL of complexes (1 mM) was added and incubated for 5 min, the fluorescence emission spectra were record by the λ_{EX}=540 nm. The concentration of ctDNA was determined by UV absorbance at 260 nm, $[ctDNA]=(Abs_{260\ nm})/(1\ cm\cdot 6600\ M^{-1}cm^{-1})$. The concentrations of complexes were 0, 0.7, 1.3, 2.0, 2.7, 3.3, 4.0, 4.7, 5.3, 6.0, 6.7 μM, respectively. The apparent binding constants were calculated following literature reported before.[23]

Absorption titration experiments

Ru complexes (20 μM) were incubated with 0, 4, 8, 12, 16, 20, 24, 28, 32, 36, 40 μM of ctDNA in Tris-HCl buffer (pH = 7.4) for 10 min at 25 °C. Then the absorption spectra were recorded.

DNA melting experiments

The DNA melting experiments were carried out on a Shimadzu UV-Vis spectrophotometer and the temperature was recorded with a platinum resistance thermometer. Equal concentration of ctDNA and Ru complexes were incubated and the absorption of the mixture was recorded at 260 nm at indicated temperature. The data was presented as $(A-A_0)/(A_f-A_0)$ *vs.* T. A = absorption at identified temperature; A_f = absorption at 56 °C; A_0 = absorption at 90 °C.

Viscosity assay

Viscosity assay was performed with an Ubbelohde viscometer at 30 °C. Ru complexes with a concentration of 0, 5, 10, 15, 20, 25, 30 μM were added into the degassed DNA solution (100 μM). Flow time (η) was recorded with a stopwatch. The data was presented as $(\eta/\eta_0)^{1/3}$ *vs.* [Complex]/[DNA].

Circular dichroism spectra

The CD spectra were obtained on a Jasco-810 spectropolarimeter. Equal amount of ctDNA and Ru complexes were mixed and equilibrated for 5 min before the spectra were recorded.

Accepted Manuscript

This article is protected by copyright. All rights reserved.

Western Blots assay

MCF-7 cells were cultured to the cell density reached 80% and cultured with **Ru1** (0.05 μM) for 4 h at 37 °C. After irradiated by 460-nm LED light (6.0 mW/cm^2) for 2 min, the cells were further incubated for 24 h. Proteins were extracted by lysis buffer. The protein concentration was measured with the BCA (bicinchoninic acid) assay on a Varioskan multimode microplate spectrophotometer (Thermo, Waltham, MA). Then proteins (20 mg/lane) in equal concentration were separated by 8-12% sodium dodecyl sulfate-polyacrylamide gel electrophoresis (SDS-PAGE), followed by transferred onto polyvinylidene difluoride (PVDF) Immobilon-P membrane (Bio-Rad) in transblot apparatus (Bio-Rad). The blots were blocked with 5% defatted milk powder in PBST (Tris-buffered saline plus 0.1% Tween 20) for 1 h, and then incubated with a series of primary antibodies against CHOP, P-eif2α, P-ERK and β-actin overnight at 4 °C. The membrane was washed with PBST (1 ml×3) and incubated with IRDye 800 conjugated secondary antibody for 1 h at 37 °C. The blots were detected by an Odyssey scanning system (Li-COR, Lincoln, Nebraska). β-actin was used as loading control.

Acknowledgements

J. Zhao and S. Gou are grateful to the National Natural Science Foundation of China (Grant Nos. 21601034 and 21571033) for financial aid for this work. This work was also supported by the Postgraduate Research & Practice Innovation Program of Jiangsu Province (KYCX18-0129). J. Zhao also thanks for the support of "Zhi-Shan" project of Southeast University. Fundamental Research Funds for the Central Universities (2242020K40031) and Priority Academic Program Development of Jiangsu Higher Education Institutions for the construction of fundamental facilities are also appreciated.

Conflict of interest

The authors declare no conflict of interest.

Keywords: Ru(II)-Polypyridyl Complex • ^{3}IL • photodynamic • DNA • ROS

[1] a) J. P. Celli, B. Q. Spring, I. Rizvi, C. L. Evans, K. S. Samkoe, S. Verma, B. W. Pogue, T. Hasan, *Chem. Rev.* **2010**, *110*, 2795-2838; b) D. Kessel, *Photodiagn. Photodyn. Ther.* **2004**, *1*, 3-7; c) M. Jakubaszek, B. Goud, S. Ferrari, G. Gasser, *Chem. Commun.* **2018**, *54*, 13040-13059; d) A. Köhler, D. Beljonne, *Adv. Funct. Mater.* **2004**, *14*, 11-18; e) J. Liu, C. Jin, B. Yuan, Y. Chen, X. Liu, L. Ji, H. Chao, *Chem. Commun.*, **2017**, *53*, 9878-9881.

[2] a) J. Liu, C. Zhang, T. W. Rees, L. Ke, L. Ji, H. Chao, *Coord. Chem. Rev.* **2018**, *363*, 17-28; b) J. Zhao, X. Zhang, L. Fang, C. Gao, C. Xu, S. Gou, *Small*. **2020**, *16*, e2000363; c) L. Wang, H. Yin, P. Cui, M. Hetu, C. Wang, S. Monro, R. D. Schaller, C. G. Cameron, B. Liu, S. Kilina, S. A. McFarland, W. Sun, *Dalton Trans.* **2017**, *46*, 8091-8103; d) C. Wang, L. Lystrom, H. Yin, M. Hetu, S. Kilina, S. A. McFarland, W. Sun, *Dalton Trans.* **2016**, *45*, 16366-16378; e) B. Liu, S. Monro, M. A. Jabed, C. G. Cameron, K. L. Colón, W. Xu, S. Kilina, S. A. McFarland, W. Sun, *Photochem. Photobiol. Sci.* **2019**, *18*, 2381-2396; f) J. Zhao, S. Sun, X. Li, W. Zhang, S. Gou, *ACS Appl. Bio. Mater.* **2020**, *3*, 252-262.

[3] S. Monro, K. L. Colón, H. Yin, J. Roque, III, P. Konda, S. Gujar, R. P. Thummel, L. Lilge, C. G. Cameron, S. A. McFarland, *Chem. Rev.* **2019**, *119*, 797-828.

[4] a) S. Ardo, G. J. Meyer, *Chem. Soc. Rev.* **2009**, *38*, 115-164; b) A. Hagfeldt, G. Boschloo, L. Sun, L. Kloo, H. Pettersson, *Chem. Rev.* **2010**, *110*, 6595-6663; c) A. Hagfeldt, M. Grätzel, *Acc. Chem. Res.* **2000**, *33*, 269-277; d) Z. Lv, L. Zou, H. Wei, S. Liu, W. Huang, Q. Zhao, ACS Appl. Mater. Interfaces. 2018, 10, 19523-19533; e) S. Bonnet, *Comments Inorg. Chem.* **2015**, *35*, 179-213; f) F. Reeßing, W. Szymanski, *Curr. Med. Chem.* **2017**, *24*, 4905-4950; g) F. Heinemann, J. Karges, G. Gasser, *Acc. Chem. Res.* **2017**, *50*, 2727-2736; h) F. E. Poynton, S. A. Bright, S. Blasco, D. C. Williams, J. M. Kelly, T. Gunnlaugsson, *Chem. Soc. Rev.* **2017**, *46*, 7706-7756; i) J. D. Knoll, B. A. Albani, C. Turro, *Chem. Commun.* **2015**, *51*, 8777-8780; j) J. K. White, R. H. Schmehl, C. Turro, *Inorg. Chim. Acta.* **2017**, *454*, 7-20; k) N. A. Smith, P. J. Sadler, Philos. *Trans. R. Soc. A* **2013**, *371*, 20120519; l) J. Zhao, S. Li, X. Wang, G. Xu, S. Gou, *Inorg. Chem.* **2019**, *58*, 2208-2217; m) J. Zhao, N. Liu, S. Sun, S. Gou, X. Wang, Z. Wang, X. Li, W. Zhang, *J. Inorg. Biochem.* **2019**, *196*, 110684; n) L.Conti, A. Bencini, C. Ferrante, C. Gellini, P. Paoli, M. Parri, G. Pietraperzia, B. Valtancoli, C. Giorgi, *Chem. Eur. J.* **2019**, *25*, 10606 – 10615; o) S. Li, J. Zhao, X. Wang, G. Xu, S. Gou, Q. Zhao, *Inorg. Chem.* **2020**, *59*, 11193−11204.

[5] a) A. E. Friedman, J. C. Chambron, J. P. Sauvage, N. J. Turro, J. K. Barton, *J. Am. Chem. Soc.* **1990**, *112*, 4960-4962; b) I. Ortmans, B. Elias, J. M. Kelly, C. Moucheron, A. K. DeMesmaeker, *Dalton Trans.* **2004**, *4*, 668-676; c) G. Li, L. Sun, L. Ji, H. Chao, *Dalton Trans.* **2016**, *45*, 13261-13276; d) B. Z. Zhu, X.-J. Chao, C.-H. Huang, Y. Li, *Chem. Sci.* **2016**, *7*, 4016-4023; e) J. Shen, H. C. Kim, J. Wolfram, C. Mu, W. Zhang, H. Liu, Y. Xie, J. Mai, H. Zhang, Z. Li, M. Guevara, Z. W. Mao, H. Shen, *Nano Lett.* **2017**, *17*, 2913-2920; f) S. Tysoe, R. Kopelman, D. Schelzig, *Inorg. Chem.* **1999**, *38*, 5196-5197.

[6] S. Kalinina, J. Breymayer, K. Reeß, L. Lilge, A. Mandel, A. Ruck, *J. Biophotonics*. **2018**, *11*, e201800085.

[7] S. Dilruba, G. V. Kalayda, *Cancer Chemother. Pharmacol.* **2016**, *77*, 1103-1124.

[8] a) H. Yin, M. Stephenson, J. Gibson, E. Sampson, G. Shi, T. Sainuddin, S. Monro, S. A. McFarland, *Inorg. Chem.* **2014**, *53*, 4548-4559; b) R. Nomula, X. Wu, J. Zhao, N. R. Munirathnam, *Mater. Sci. Eng. C* **2017**, *79*, 710-719.

[9] C. S. Burke, A. Byrne, Tia. E. Keyes, *J. Am. Chem. Soc.* **2018**, *140*, 6945-6955.

[10] Y. Sun, L. E. Joyce, N. M. Dickson, Claudia Turro, *Chem. Commun.* **2010**, *46*, 2426-2428.

[11] a) V. Pierroz, R. Rubbiani, C. Gentili, M. Patra, C. Mari, G. Gasser, Stefano Ferrari, *Chem. Sci.* **2016**, *7*, 6115-6124; b) C. Mari, V. Pierroz, R. Rubbiani, M. Patra, J. Hess, B. Spingler, L. Oehninger, J. Schur, I. Ott, L. Salassa, S. Ferrari, Gilles Gasser, *Chem. Eur. J.* **2014**, *20*, 14421-14436; c) J. Hess, H. Huang, A. Kaiser, V. Pierroz, O. Blacque, H. Chao, Gilles Gasser, *Chem. Eur. J.* **2017**, *23*, 9888-9896; d) C. Mari, V. Pierroz, A. Leonidova, S. Ferrari, G. Gasser, *Eur. J. Inorg. Chem.* **2015**, *23*, 3879-3891; e) J. P. Hall, S. P. Gurung, J. Henle, P. Poidl, J. Andersson, P. Lincoln, G. Winter, T. Sorensen, D. J. Cardin, J. A. Brazier, C. J. Cardin, *Chem. Eur. J.* **2017**, *23*, 4981-4985; f) J. P. Hall, H. Beer, K. Buchner, D. J. Cardin, C. J. Cardin, *Organometallics*. **2015**, *34*, 2481-2486.

[12] a) T. A. Grusenmeyer, J. Chen, Y. Jin, J. Nguyen, J. J. Rack, R. H. Schmehl, *J. Am. Chem. Soc.* **2012**, *134*, 7497−7506; b) C. Reichardt, K. R. A. Schneider, T. Sainuddin, M. Wächtler, S. A. McFarland, B. Dietzek, *J. Phys. Chem. A* 2017, 121, 5635−5644; c) M. Mariappan, B. G. Maiya, *Eur. J. Inorg. Chem.* **2005**, *11*, 2164–2173; d) S. Mardanya, S. Karmakar, D. Mondal, S. Baitalik, *Inorg. Chem.* **2016**, *55*, 3475−3489; e) M. Mariappan, A. Ramasamy, P. A. Prasanth, V. Anbazhagan, R. Senthilnathan, A. Jothi, *J. Photoch. Photobio. A.* **2018**, *356*, 617-626.

Accepted Manuscript

This article is protected by copyright. All rights reserved.

[13] a) G. Ghosh, K. L. Colón, A. Fuller, T. Sainuddin, E. Bradner, J. McCain, S. M. A. Monro, H. Yin, M. W. Hetu, C. G. Cameron, S. A. McFarland, *Inorg. Chem.* **2018**, *57*, 7694−7712; b) J. McCain, K. L. Colón, P. C. Barrett, S. M. A. Monro, T. Sainuddin, J. Roque III, M. Pinto, H. Yin, C. G. Cameron, S. A. McFarland, *Inorg. Chem.* **2019**, *58*, 10778−10790; c) T. C. Motley, L. Troian-Gautier, M. K. Brennaman, G. J. Meyer, *Inorg. Chem.* **2017**, *56*, 13579−13592.

[14] T. Sainuddin, J. McCain, M. Pinto, H. Yin, J. Gibson, M. Hetu, S. A. McFarland, *Inorg. Chem.* **2016**, *55*, 83-95.

[15] S. J, W. Wu, W. Wu, P. Song, K. Han, Z. Wang, S. Liu, H. Guo, J. Zhao, *J. Mater. Chem.* **2010**, *20*, 1953-1963.

[16] a) Y. Liu, R.Hammitt, D. A. Lutterman, L. E. Joyce, R. P. Thummel, C. Turro, *Inorg. Chem.* **2009,** *48*, 375-385; b) S. P. Foxon, C. Metcalfe, H. Adams, M. Webb, J. A. Thomas, *Inorg. Chem.* **2007**, *46*, 409-416; c) S. P. Foxon, M. A. H. Alamiry, M. G. Walker, A. J. H. M. Meijer, I. V. Sazanovich, J. A. Weinstein, J. A. Thomas, *J. Phys. Chem. A* **2009**, *113*, 12754-12762; d) L. Wang, H. Yin, M. A. Jabed, M. Hetu, S. Monro, C. Wang, S. Kilina, S. A. McFarland, W. Sun, *Inorg. Chem.* **2017**, *56*, 3245-3259.

[17] C. Reichardt, S. Monro, F. H. Sobotta, K. L. Colón, T. Sainuddin, M. Stephenson, E. Sampson, J. Roque III, H. Yin, J. C. Brendel, C. G. Cameron, S. McFarland, B. Dietzek, *Inorg. Chem.* **2019**, *58*, 3156-3166.

[18] K. Suzuki, A. Kobayashi, S. Kaneko, K. Takehira, T. Yoshihara, H. Ishida, Y. Shiina, S. Oishic, S. Tobita, Phys. *Chem. Chem. Phys.* **2009**, *11*, 9850-9860.

[19] F. Vogtle, M. Plevoets, M. Nieger, G. C. Azzellini, A. Credi, L. De Cola, V. De Marchis, M. Venturi, V. Balzani, *J. Am. Chem. Soc.* **1999**, *121*, 6290-6298.

[20] K. Bhattacharyya, P. K. Das, *Chem. Phys. Lett.* **1985**, *116*, 326-332.

[21] F. L. Zhang, M. R. Song, G. K. Yuan, H. N. Ye, Y. Tian, M. D. Huang, J. P. Xue, Z. H. Zhang, J. Y. Liu, *J. Med. Chem.* **2017**, *60*, 6693-6703.

[22] P. Khanvilkar, R. Pulipaka, K. Shirsath, R. Devkar, D. Chakraborty, *J. Coord. Chem.* **2019**, *72*, 2617-2635.

[23] M. J. Han, Z. M. Duan, Q. Hao, S. Z. Zheng, K. Z. Wang, *J. Phys. Chem. C* **2007**, *111*, 16577-16585.

[24] G. M. Morris, R. Huey, W. Lindstrom, M. F. Sanner, R. K. Belew, D. S. Goodsell, A. J. Olson, *J. Comput. Chem.* **2009**, *30*, 2785-2791.

[25] a) M. P. Murphy, *Biochem. J.* **2009**, *417*, 1-13; b) H. U. Simon, A. Haj-Yehia, F. Levi-Schaffer, *Apoptosis*. **2000**, *5*, 415-418; c) K. B. Huang, F. Y. Wang, X. M. Tang, H. W. Feng, Z.F. Chen, Y. C. Liu, Y. N. Liu, H. Liang, *J. Med. Chem.* **2018**, *61*, 3478-3490.

[26] Z. Zhou, J. Liu, T. W. Rees, H. Wang, X. Li, H. Chao, P. J. Stang, *Proc. Natl. Acad. Sci. U. S. A.* **2018**, *115*, 5664-5669.

WILEY-VCH

Accepted Manuscript

This article is protected by copyright. All rights reserved.

10.1002/chem.202003031

WILEY-VCH

Entry for the Table of Contents (Please choose one layout)

Layout 1:

FULL PAPER

DNA targeting Ru(II)-polypyridyl complex with potent phototoxcity intercalate into DNA, cause sever DNA damage and activate ER stress.

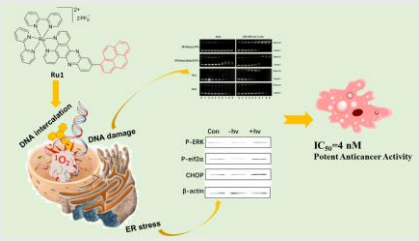

*Author(s), Corresponding Author(s)**

Page No. – Page No.

Title

Layout 2:

FULL PAPER

((Insert TOC Graphic here; max. width: 11.5 cm; max. height: 2.5 cm))

*Author(s), Corresponding Author(s)**

Page No. – Page No.

Title

Text for Table of Contents

Accepted Manuscript

This article is protected by copyright. All rights reserved.